Optimisation of high-speed lipidome analysis by nanoflow ultrahigh-performance liquid chromatography-tandem mass spectrometry: Application to identify candidate biomarkers for four different cancers

Gwang Bin Lee, Young Beom Kim, Jong Cheol Lee, Myeong Hee Moon[*]

Department of Chemistry, Yonsei University, 50 Yonsei-ro, Seoul 03722, South Korea

ABSTRACT

Lipid analysis is a powerful tool that can elucidate the pathogenic roles of lipids in metabolic diseases, and facilitate the development of potential biomarkers. Lipid analysis by large-scale lipidomics requires a high-speed and high-throughput analytical platform. In the present study, a high-speed analytical method for lipid analysis using nanoflow ultrahigh-performance liquid chromatography-electrospray ionisation-tandem mass spectrometry (nUHPLC-ESI-MS/MS) was optimised by investigating the effects of column flow rate, pump flow rate, dwell time, initial binary mobile phase composition, and gradient duration on the separation efficiency of standard lipid mixtures. The minimum gradient time for high-speed lipid separation was determined by examining the time-based separation efficiency and spectral overlap of isobaric lipid species during selected reaction monitoring-based quantification of sphingomyelin and a second isotope of phosphatidylcholine, which differ in molecular weight by only 1 Da. Finally, the optimised nUHPLC-ESI-MS/MS method was applied to analyse 200 plasma samples from patients with liver, gastric, lung, and colorectal cancer to evaluate its performance by measuring previously identified candidate lipid biomarkers. About 73% of the reported marker candidates (6 out of 7 in liver, 5/9 in gastric, 4/6 in lung, and 6/7 in colorectal cancer) could be assigned using the optimised method, supporting its use for high-throughput lipid analysis.

1. Introduction

Lipids are the major components of cell membranes; they are involved in energy storage, signal transmission, cell growth, and programmed cell death [1-3]. Perturbations in lipid profiles are associated with the progression of metabolic diseases, such as diabetes, cardiovascular disease, and cancer [3-7]. Analysis of lipid profiles has contributed greatly to understand the pathogenic roles of lipids and to develop potential biomarkers for diseases. Going forward, large-scale lipidomics is expected to provide new perspectives on the pathophysiological mechanisms of disease and aid clinical decision-making in personalised medicine [8].

Lipids are complex mixtures that can be classified into eight different categories: fatty acids, sterols, glycerolipids (GLs), glycerophospholipids (GPLs), sphingolipids (SLs), saccharolipids, prenols, and polyketides [9]. Because of this complexity, lipidome analysis often requires a systematic analytical platform to carry out untargeted identification of lipids, followed by targeted quantitation. While sophisticated mass spectrometry

(MS)-based methods offer excellent characterisation of lipid molecular structures and lipid quantification, liquid chromatography (LC) is essential to separate lipids in their intact state prior to MS-based detection in order to minimise ion suppression effects [10-12]. A high-throughput and high-speed analytical protocol that covers broad lipid classes without causing spectral congestion is therefore required to acquire accurate large-scale lipidomic data from biological samples. Recent studies have shown that the coverage of identified lipids is related to the analysis time [8]. While a number of studies have reported that 20–30 min is the minimum analysis time required for high lipid coverage, few have adopted a high speed (<10 min analysis time) targeted approach at the cost of lipid coverage [13-19]. The speed of lipid separation has been greatly improved by the implementation of ultrahigh-performance LC (UHPLC) coupled with MS [20,21]. However, there is a possibility of spectral overlap between isobaric species when quantification is based on the selected reaction monitoring (SRM) of a limited number of fragment ions. Because the analysis time per run is critical for expediting large-scale lipidomic analysis, it is important to

investigate the relationship between the speed of analysis and the efficiency of lipid identification and quantification. Nanoflow UHPLC with electrospray ionisation-tandem mass spectrometry (nUHPLC-ESI-MS/MS) offers several advantages, including increased separation efficiency, precision with regard to retention time, and the minimisation of the amounts of sample (~microgram scale) and organic solvents used per run [22-25]. However, the duration of each run with nUHPLC is usually approximately 30 min for a typical global lipid analysis, and this needs to be optimised to increase the efficiency of the analysis.

In the present study, a rapid analysis of nUHPLC-ESI-MS/MS method was optimised for high-throughput lipidomics. Experimental variables, including flow rates for both the pump and column, gradient duration, and initial solvent composition of the gradient were investigated using lipid standards to maximise the speed of separation without compromising efficiency. The effect of gradient time on lipid separation was examined by investigating the possible spectral overlap of isobaric species from different lipid classes during SRM-based quantification and the time-based separation efficiency in lipid separation. The optimised method for lipidome analysis was applied to the high-speed, SRM-based targeted quantitative analysis of 200 blood plasma samples for the confirmation of lipid biomarker candidates for four different cancers (liver, gastric, lung, and colorectal) that were reported in a previous study [7]. Candidate lipid markers that were selected as those specific to one or multiple cancer types were examined for the confirmation of the accuracy and efficiency of the optimised method. A rapid and accurate quantitative method for lipid profiling has potential applications in the clinical setting, where it could assist decision-making processes in personalised medicine.

2. Materials and methods

2.1. Materials and reagents

For the optimisation of nUHPLC-ESI-MS/MS run conditions, 53 lipid standards were purchased from Avanti Polar Lipids Inc. (Alabaster, AL, USA), as follows: Lysophosphatidylcholine (LPC) 16:0, LPC 17:0, LPC 17:1, LPC 18:1-D7, phosphatidylcholine (PC) 12:0/12:0, PC 16:0/16:0, PC 17:0/17:0, PC 15:0/18:1-D7, PC-plasmalogen (PC) P-18:0/22:6, lysophosphatidylethanolamine (LPE) 14:0, LPE 17:1, LPE 18:0, LPE 18:1-D7, phosphatidylethanolamine (PE) 16:0/16:0, PE 17:0/17:0, PE 15:0/18:0-D7, PE plasmalogen (PE) P-18:0/22:6, PE P-18:0/18:1-D9, lysophosphatidic acid (LPA) 17:0, LPA 17:1, lysophosphatidylglycerol (LPG) 13:0, LPG 14:0, LPG 17:1, LPG 18:0, phosphatidylglycerol (PG) 15:0/15:0, PG 16:0/16:0, PG 17:0/17:0, PG 15:0/18:1-D7, lysophosphatidylinositol (LPI) 13:0, LPI 17:1, phosphatidylinositol (PI) 16:0/18:1, PI 16:0-D31/18:1, PI 15:0/18:1-D7, sphingomyelin (SM) d18:1/16:0, SM d18:1/17:0, SM d18:1/18:1-D9, ceramide (Cer) d18:1/14:0, Cer d18:1/22:0, Cer d18:1-D7/24:0, Cer d18:1-D7/24:1, mono-hexosylceramide (HexCer) d18:1/12:0, HexCer d18:1/16:0, HexCer d18:1/17:0, HexCer d18:1-D7/15:0, sulfatide (SulfoHexCer) d18:1-D7/13:0, SulfoHexCer d18:1/17:0, SulfoHexCer d18:1/24:0, diacylglycerol (DG) 16:0_18:1, DG 1,3–18:0-D5, DG 15:0_18:1-D7, triacylglycerol (TG) 17:0/17:1/17:0-D5, TG 15:0/18:1-D7/15:0, and cardiolipin (CL) (14:0)$_4$. Non-endogenous lipids containing odd-numbered acyl chains were used as external standards for calibration, and standard lipids containing deuterated acyl chains were used as internal standards, which were spiked into each plasma sample before lipid extraction for SRM quantitation. All organic solvents (CH_3CN, CH_3OH, isopropyl alcohol (IPA), and methyl-*tert*-butyl ether (MTBE)) and water that were used for HPLC mobile phase and lipid extraction were of HPLC grade and procured from Avantor Performance Materials (Center Valley, PA, USA). NH_4HCO_2, NH_4OH, and $CHCl_3$ were purchased from Sigma-Aldrich (St. Louis, MO, USA). Silica capillary tubes (inner diameters of 20, 50, and 100 μm, and an outer diameter of 360 μm) purchased from Polymicro Technology LLC (Phoenix, AZ, USA) were used to prepare the capillary LC columns and to connect the UHPLC pump and capillary column. Two stationary phases were used to generate custom columns: 3 μm, 100 Å Watchers ODS-P C-18 beads from Isu Industry Corp. (Seoul, Korea) to form a self-assembled frit of 0.5 cm at the column tip, and 1.7 μm, 130 Å ethylene bridged hybrid (BEH) beads unpacked from an ACQUITY UHPLC BEH C18 column (2.1 mm × 100 mm) from Waters (Milford, MA, USA) for the main column, packed after the self-assembled frit.

2.2. Human plasma samples

A total of 200 human blood plasma samples were examined in the present study: 50 healthy controls, 50 liver cancer, 50 gastric cancer, 25 lung cancer, and 25 colorectal cancer samples. Healthy control samples were provided by the Ajou University Hospital Biobank (Suwon, Korea), a member of the Korea Bioresources Network (KBN). Samples from patients diagnosed with different cancers were provided by the Biobank of Severance Hospital at Yonsei University (Seoul, Korea). This study was approved by the Institutional Review Board of Severance Hospital and was conducted in accordance with the current version of the Declaration of Helsinki. The demographic information of each sample group is listed in supplementary Table S1. The plasma samples were stored at −80 °C until lipid extraction.

2.3. Lipid extraction

Extraction of plasma lipids was performed using MTBE/CH_3OH according to a previously published method [26]. A 50-μL aliquot of each plasma sample was dried in a Bondiro MCFD 8508 freeze dryer vacuum centrifuge (ilShinBioBase, Yangju, Korea). Each lyophilised plasma sample was mixed with 300 μL of CH_3OH and incubated for 10 min in an ice bath. The plasma-methanol solution was mixed with 1000 μL of MTBE followed by vortexing for 1 h. MS-grade water (250 μL) was added to the mixture, followed by vortexing for 10 min and centrifugation at 1000 *g* for 10 min. The upper organic layer containing lipids was pipetted into a clean centrifuge tube. The remaining lipids were retrieved from the lower aqueous layer by the addition of 300 μL of MTBE and tip-sonication for 2 min. After centrifuging the mixture at 1000 *g* for 10 min, the resulting supernatant organic layer was merged with the previously collected organic layer. For the removal of organic solvents in the final mixture, the vial was sealed with 0.45-μm MilliWrap PTFE membrane (Millipore, Burlington, MA, USA) and dried in a vacuum centrifuge. Dried lipid powders were dissolved in 200 μL of $CHCl_3$:CH_3OH:H_2O (1:18:1, v/v/v). The lipid solution was stored at −80 °C until analysis.

2.4. Lipid analysis by nUHPLC-ESI-MS/MS

Lipid analysis was carried out on a nanoACQUITY UPLC system from Waters (Milford, MA, USA) in-line with a TSQ Vantage triple-stage quadrupole MS system (Thermo Scientific, San Jose, CA, USA). Targeted SRM quantitation was based on lipid molecules selected as candidate markers for different cancers in a previous study [7]. The analytical column was a fused silica capillary column (inner diameter, 100 μm; outer diameter, 360 μm) prepared in-house, in which the tip of the capillary was pulled into a sharp needle with a flame and used as the emitter for ESI. The capillary column was packed in two stages: the first 0.5 cm of the needle tip was filled with Watchers® 3 μm ODS-P C18 beads to form a self-assembled frit, and the remaining 7.5 cm was packed with 1.7 μm −130 Å XBridge BEH C18 beads (Waters) under nitrogen gas at 1000 psi. The capillary column was connected to the UHPLC pump with NanoViper™ fittings from Thermo Scientific (San Jose, CA) and a stainless steel microcross from IDEX (Oak Harbor, WA) as shown in supplementary Fig. S1. The additional two ports were connected to a Pt wire for the ESI voltage source and a narrow-bore tube (20 μm i.d. and 350 mm nanoViper) to provide pressure for splitting the pump flow into a nano flow for the analytical column. The pressure tube was connected to an on/off switching valve for two modes: blocked or
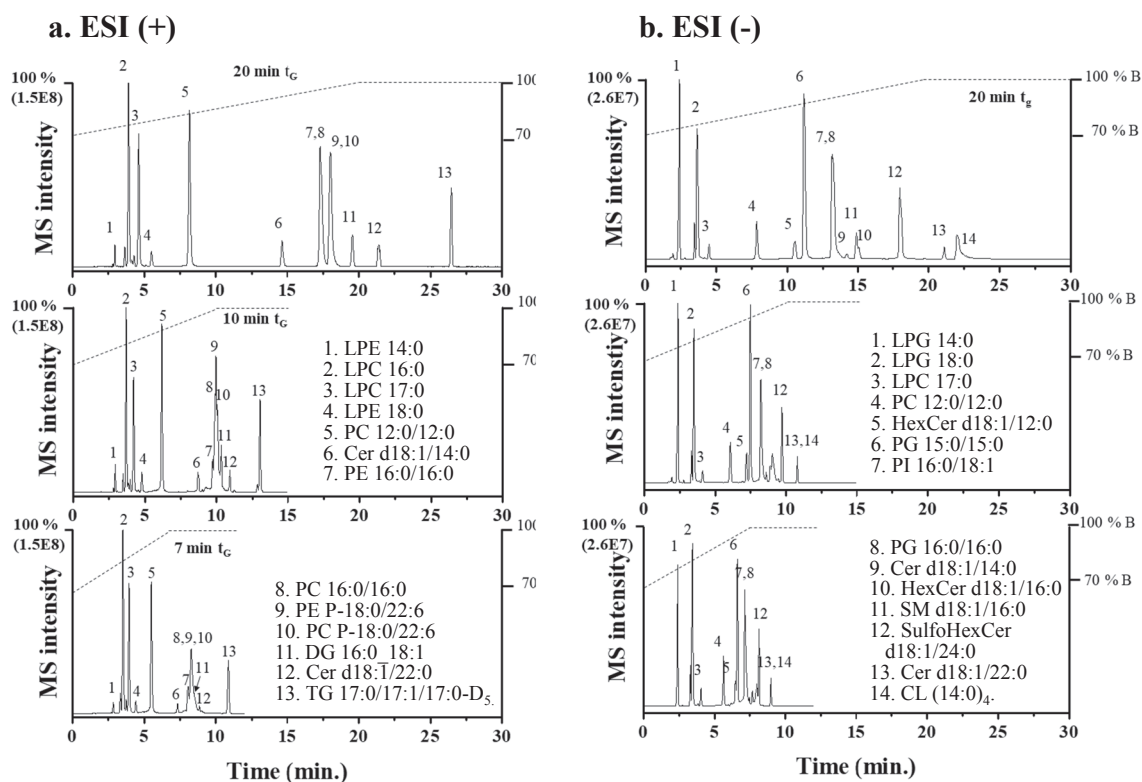
Fig. 1. Effect of gradient time (t$_G$) on the separation of lipid standards in (a) positive and (b) negative ion modes of nUHPLC-ESI-MS/MS.

split flow. The mobile phase solutions used for binary gradient elution were (9:1, v/v) H$_2$O:CH$_3$CN for A and (2:2:6, v/v/v) CH$_3$OH:CH$_3$CN:IPA for B. The mobile phases were combined with a mixture of ionisation modifiers (0.5 mM NH$_4$HCO$_2$ and 7.4 mM NH$_4$OH), which are efficient for both positive and negative ion modes during MS analysis. The lipid sample was loaded with 100% mobile phase A at 800 nL/min for 10 min with the on–off switching valve blocked. Gradient elution was begun by increasing the level of mobile phase B from 70% to 100% over 10 min, followed by 5 min of 100% B. The pump flow rate during gradient elution was adjusted to 16 μL/min with the on/off valve in the 'on' position, so that the column flow rate was adjusted to 0.65 μL/min. Then, the level of mobile phase B was reduced to 0% for 5 min to recondition the column. The ESI voltage applied to the emitter was 3 kV and 1.5 kV in the positive and negative ion mode, respectively.

During SRM quantitation, lipid ions were detected using the polarity switching mode in which detection was made in the positive and negative ion modes alternatively in a single run, using a scan width of m/z 1.0, and a scan time of 0.001 s. Each lipid species was detected by a precursor ion and its specific product ion (quantifier ion). The precursor and product ions for each lipid class are listed in Table S2, along with the specific collision energy applied for each lipid class. SPLASH® LIP-IDOMIX® Mass Spec Standard (Avanti Polar Lipids Inc.), a mixture of lipid standards, was spiked into each plasma sample as an internal standard (IS) prior to lipid extraction, as listed in Table S2. The lipid classes LPC, PC, LPE, PE, EtherPE, SM, Cer, HexCer, SulfoHexCer, DG, and TG were detected in the positive ion mode. The classes LPA, LPG, PG, LPI, and PI were detected in the negative ion mode. Statistical analysis was performed using the SPSS software (version 24.0, IBM Corp., Armonk, NY, USA) for one-way analysis of variance (ANOVA) and logistic regression, and the Minitap 17 statistical software (http://www.minitap.co.kr) for principal component analysis (PCA).

2.5. Method validation

The lipid quantification method was validated by analysing plasma

samples spiked with a set of internal and external lipid standards, listed in Table S3, by varying the injection amounts of internal standards (72–1948 fmol) and external standards (30–4000 fmol). The limit of detection (LOD) and the limit of quantitation (LOQ) were based on the calibration curves established from the peak area of standard lipids as the signal-to-noise ratio (S/N) = 3 and 10, respectively. The LOD values based on the formula 3 × (standard deviation of y-intercept) / slope of calibration curve) were in the range of 5.2 (TG 17:0/17:1/17:0-D5)– 27.7 fmol (EtherPE P-18:0/18:1-D9) and LOQ values (S/N = 10) were in the range of 17.3–92.4 fmol. The calibration curves were plotted using the peak areas of each lipid class at 9 different concentrations; 30, 50, 100, 300, 500, 800, 1000, 2000, and 4000 fmol. The LOD and LOQ values of the 16 lipid classes are listed in Table S3.

3. Results and discussion

3.1. Optimisation of nUHPLC-ESI-MS/MS for high-speed lipid quantification

Lipidome analysis by LC-ESI-MS/MS is commonly performed with the reversed phase using binary gradient elution. When a simultaneous analysis of lipids with broad lipid classes is required, it is essential to properly select the initial mobile phase (MP) composition, pump flow rate, column flow rate, and the gradient duration (t$_G$) to maximise the number of identified lipids, along with the separation speed and the accuracy of quantification. In Fig. 1, typical nUHPLC-ESI-MS/MS analysis of lipids was demonstrated by the separation of lipid mixtures covering a broad range of hydrophobicities: from lysophosphatidylcholine (LPC) to triacylglycerol (TG) in positive ion mode at the top of Fig. 1a and from lysophosphatidylglycerol (LPG) to cardiolipin (CL) in the negative ion mode at the top of Fig. 1b. Both runs were performed with t$_G$ = 20 min at a column flow rate of 0.65 μL/min. With a gradient duration of 20 min, a high resolution and high precision separation of lipids was achieved, with an average peak width of 0.25 min and a relative error in retention times of 0.67% (n = 5) for the lipid standards
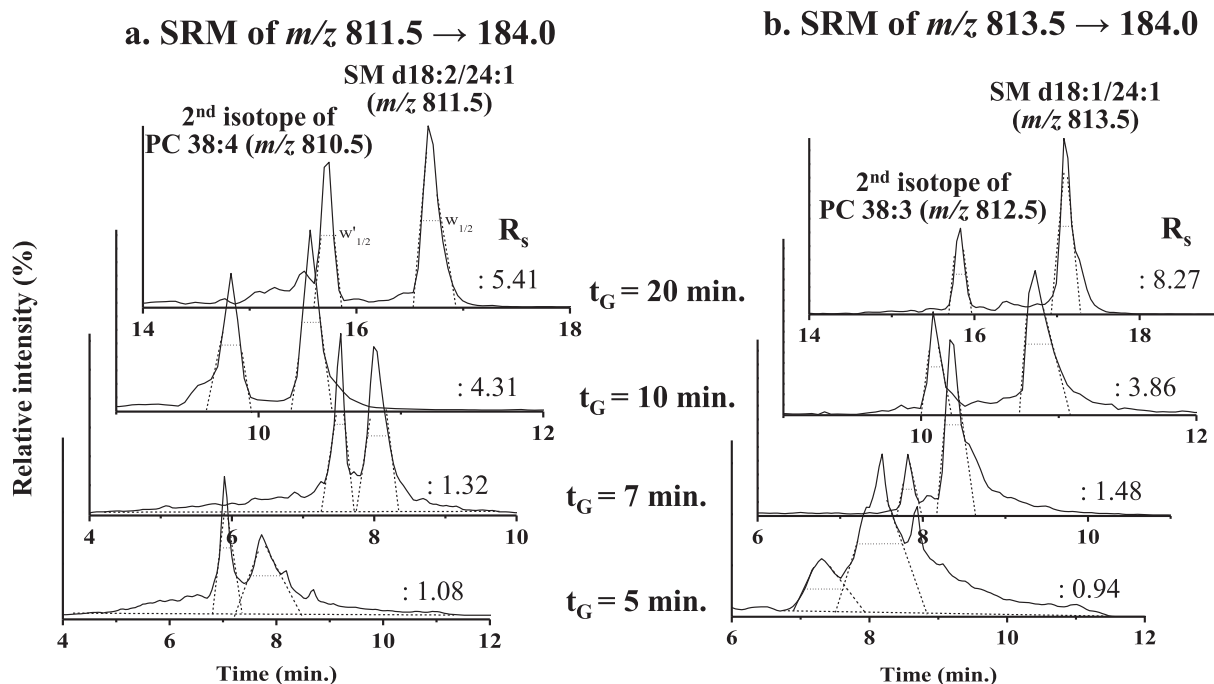
Fig. 2. Effect of gradient time (t_G) on the selected reaction monitoring (SRM) quantification of isobaric lipid species by nUHPLC-ESI-MS/MS. Extracted ion chromatograms were obtained by SRM transition of (a) m/z 811.5 → 184.0 representing the simultaneous detection of 2nd isotope of PC 38:4 (m/z 810.5) and SM d18:2/24:1 (m/z 811.5), and (b) m/z 813.5 → 184.0 detecting 2nd isotope of PC 38:3 (m/z 812.5) and SM d18:1/24:1 (m/z 813.5).

in both base peak chromatograms (BPCs). To expedite lipid separation for large-scale lipidomic analysis, t_G was reduced to 10, 7, and then to 5 min. The entire analysis time can be reduced to as little as 12 min, but a serious overlap in ions was observed in runs obtained at t_G = 7 min (Fig. 1). While the runs with different gradient durations in Fig. 1 began with the same initial MP composition (70% B (2:2:6 CH$_3$OH:CH$_3$CN:IPA) ramped to 100% B), the effect of initial MP composition on lipid separation was examined by varying the initial composition of B (2:2:6 CH$_3$OH:CH$_3$CN:IPA) from 30 to 70% with t_G = 10 min, as shown in supplementary Fig. S2. Lipids can elute over a 10 min of time interval with less serious peak overlaps under the 70% B initial MP condition both positive and negative ion modes.

The effect of dwell time on lipid separation was also investigated by varying the pump flow rate (8 or 16 μL/min), while the column flow rate remained at 0.65 μL/min (supplementary Fig. S3). This can be easily made by splitting the pump flow before the column as shown in supplementary Fig. S1. With increased pump flow rate, changes in MP composition are more promptly conveyed to the column during gradient elution. The peak intensities of highly retained lipid species, such as Cer d18:1/22:0 (peak No. 12) and TG 17:0/17:1/17:0-D5 (No. 13), were significantly increased by 28% and 672%, respectively, with a higher pump flow rate of 16 μL/min (supplementary Fig. S3a), while the retention time was slightly reduced. Peak capacity increased to 81.2 from 59.0 for TG 17:0/17:1/17:0-D5 and to 43.8 from 25.1 for CL(14:0)$_4$ under a higher pump flow rate. Calculation of peak capacity (n_c) was based on the peak capacity of gradient chromatography, $n_c = 1 + t_G/4\sigma$ where 4σ is peak width [27]. This indicates that the reduction in dwell time was essential to reduce band broadening effects during the gradient elution of lipids by nUHPLC. A further increase in the pump flowrate was not attempted because of the difficulty in splitting higher flow to accurately control the column flow rate.

The effect of column flow rate on the separation efficiency was examined at two different flow rates (0.3 and 0.65 μL/min), while the pump flow rate was fixed at 16 μL/min (supplementary Fig. S4), resulting in the separation time being reduced by 10% with increased peak recovery of the long retaining species(peaks no. 12–14) at 0.65 μL/

min. Moreover, the observed peak capacity increased to 81.2 from 60.5 for TG 17:0/17:1/17:0-D5 and 43.8 from 19.5 for CL(14:0)$_4$ when the column flow rate was set to 0.65 μL/min.

There are two challenging issues to overcome when separating lipids on a short gradient: peak overlap of isobaric lipid species from different classes and decreased separation efficiency. Quantitative analysis by SRM uses a precursor and its product ion for the selective detection and quantitation of a specific molecule. PC and SM have the same phosphocholine head group, but different backbone molecules (two fatty acyl chains in a glycerol structure for PC and one fatty acyl chain in sphingosine for SM), and so, they can be distinguished by their precursor and product ions obtained from the dissociation of acyl chains by collision-induced dissociation (CID). However, in the case of an SM species and the second isotope of a PC with a precursor mass of 1 Da less than that of the SM, they cannot be distinguished by SRM-based quantification when their retention times are very close to each other. Most lipid classes are quantified with typical product ions derived from the dissociation of acyl chains, including free carboxylate ions ([RCOO]$^-$) in negative ion mode, or the remaining product ion after the loss of acyl chain ([M + H-RCOOH]$^+$) in positive ion mode, as listed in supplementary Table S2. However, quantification of PC and SM classes relies only on a single quantifier ion, [Pcho + H]$^+$, which is a phosphocholine ion, making it challenging to distinguish isobaric species of different classes when proper separation of the two lipid molecules is not achieved. In the case of SRM-based quantification of a lipid extract from human plasma, SM d18:2/24:1 (m/z 811.5) and the second isotope of PC 38:4 (m/z 810.5), where the m/z of the second isotope of PC 38:4 is the same as SM d18:2/24:1, are simultaneously detected by the SRM transition of m/z 811.5 → 184.0 ([Pcho + H]$^+$), as illustrated in Fig. 2. When t_G was reduced from 20 min to 5 min (Fig. 2a), the extracted ion chromatograms showed that the peaks of the two isobaric species were separated at the baseline level until t_G = 10 min, with differences in retention times (9.81 vs. 10.36 min). When t_G was reduced to 7 min, the two isobaric species eluted with an incomplete baseline separation at a resolution (R_s) of 1.32. A further decrease to t_G = 5 min resulted in a decrease in resolution to 1.08. The last two run conditions were therefore not suitable for quantitative
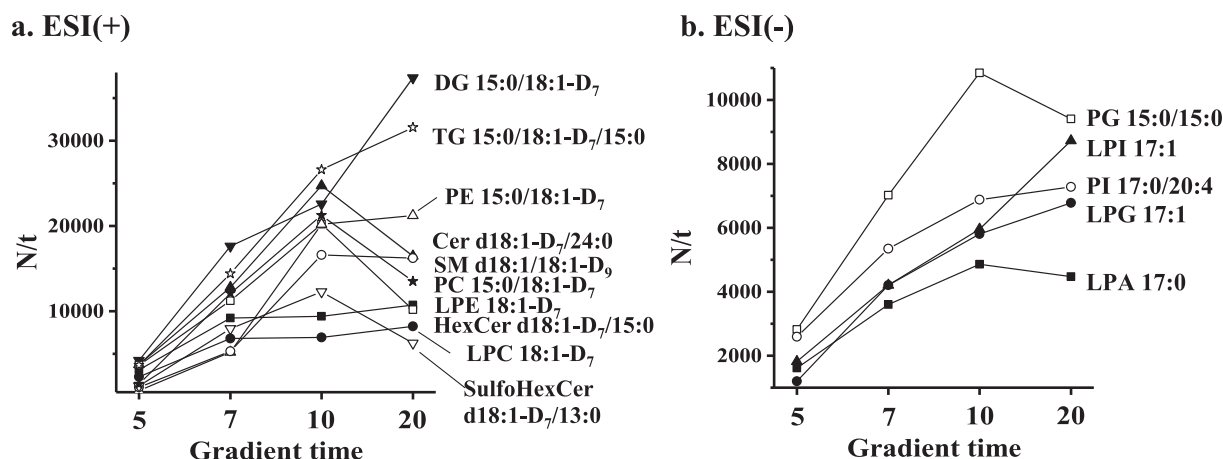
Fig. 3. The peak capacity (n_c) upon the different gradient times (t_G) observed for 15 lipid standards at (a) positive and (b) negative ion modes of nUHPLC-ESI-MS/MS.
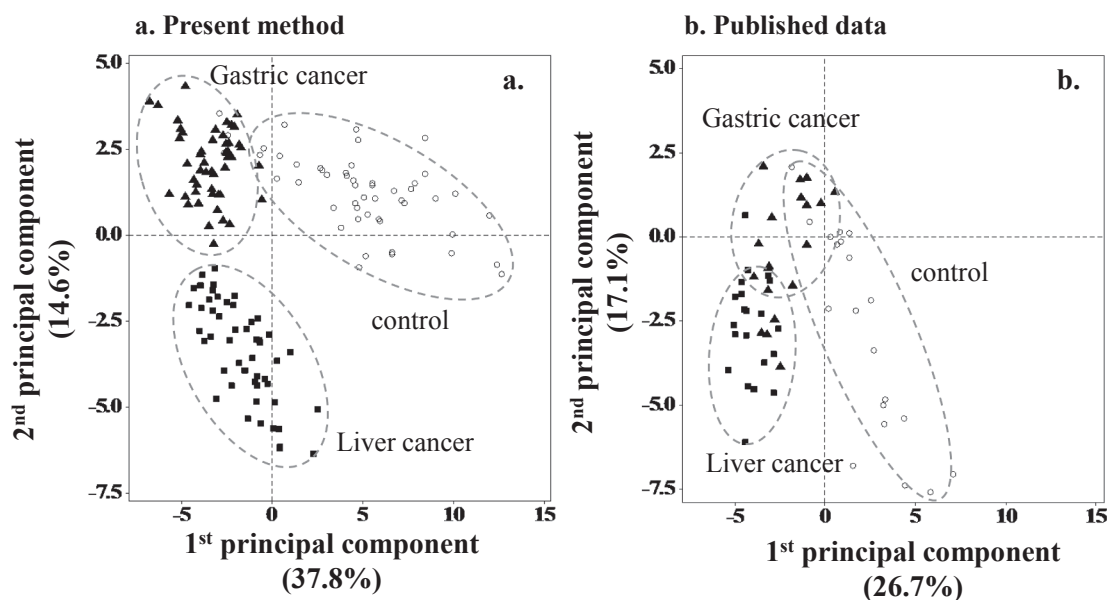

Fig. 4. Comparison of principal component analysis (PCA) plots obtained between a) the high-speed analysis and b) the previous reports. PCA was carried out with plasma lipids showing a significant difference (>2.0-fold and $p < 0.05$) either in liver cancer (n = 50) or gastric cancer (n = 50) compared with controls (n = 50). Plot b was regenerated with permission from the raw data of [7].

calculations (which require at least $R_s > 1.5$). A serious peak overlap with a loss of resolution was observed in the case of a second isotope of PC 38:3 (m/z 812.5) and SM d18:1/24:1 (m/z 813.5) (Fig. 2b) when t_G was reduced to 5 min. Fig. 2 demonstrates the importance of the balance between separation speed and the loss of resolution for SRM-based quantification of lipids when high-speed separation is required.

An effort to optimise t_G was further evaluated by estimating peak capacity and time-based separation efficiency [28] of each lipid standard, by calculating the observed plate number relative to its retention time (N/t) at different values of t_G (Fig. 3). Since the peak capacity values continuously decreased with the decrease of the gradient time (Fig. S5), it was difficult to optimize the speed of separation in terms of efficiency. When N/t was plotted against each gradient time (Fig. 3), the time-based separation efficiency of most lipid species was maximised at $t_G = 10$ min, except for DG and TG in positive ion mode and LPI and LPG in negative ion mode. By considering the influence of the experimental parameters examined so far, an optimised run condition of $t_G = 10$ min with an initial 70% B MP composition at 0.65 µL/min column flow rate and 16 µL/min pump flow rate was selected for high-speed lipid

quantification and was next evaluated using blood plasma samples from patients with different cancer types.

3.2. Application of optimised method to quantify plasma lipids in patients with cancer

The optimised run conditions for nUHPLC-ESI-MS/MS analysis of lipids reduced the initial analysis time by approximately two-fold, from ~ 27 min with $t_G = 20$ min to ~ 13 min with $t_G = 10$ min in positive ion mode. For SRM-based quantification, the entire analysis time for lipidome samples can be further reduced by two-fold if MS detection is performed with polarity switching, in which eluted lipids are alternately detected in positive and negative ion modes in a single run. In this study, the optimised run conditions were applied for the quantification of plasma lipids from patients with four different cancer types (liver, gastric, lung, and colorectal cancers). A total of 152 lipids with concentrations above the LOQ were identified, and the relative peak area (vs. IS), relative abundance in each lipid class, and fold ratio (vs. controls) of each lipid in both liver and gastric cancers are presented in

Table 1

Comparison of the fold ratio values (cancer vs. control) of the selected lipids obtained by the present work with those reported in the previous study. Lipids were selected by the screening criteria showing significant differences (>2.0-fold vs. controls and $p < 0.05$) in the previous study in human blood plasma samples with liver cancer and gastric cancer. Species marked with bold was selected in the previous study [7] as candidate lipid marker specific to each cancer based on ROC analysis (AUC > 0.800). Statistical p values were <0.01 for all species except for * ($p < 0.05$) and † ($p > 0.05$). Data from Ref. were reprinted with permission from [7]. Copyright 2019 Elsevier B.V.

Class	Molecular species	m/z	Fold ratio in Liver cancer		Fold ratio in Gastric cancer	
			Ref. [7]	The present study	Ref. [7]	The present study
LPC	16:0	496.5	**4.55 ± 0.82**	**1.43 ± 0.05**	4.58 ± 0.80	1.52 ± 0.06
	18:2	520.5	**4.77 ± 1.10**	**1.69 ± 0.07**	3.59 ± 0.71*	1.95 ± 0.12
PC	34:2	758.5			0.49 ± 0.03	0.48 ± 0.02
	36:3	784.5			0.50 ± 0.10	0.45 ± 0.01
	36:4	782.5			0.48 ± 0.16	0.49 ± 0.01
LPE	16:0	454.5	0.29 ± 0.08	0.43 ± 0.05	**0.29 ± 0.08**	**0.52 ± 0.07**
	18:0	482.5	0.27 ± 0.08	0.40 ± 0.05	**0.48 ± 0.12**	**0.57 ± 0.07**
	18:1	480.5	0.10 ± 0.03	0.30 ± 0.04	**0.19 ± 0.06**	**0.53 ± 0.07**
	18:2	478.5	0.16 ± 0.04	0.28 ± 0.03		
PE	34:1	718.5	0.48 ± 0.14	0.79 ± 0.07†		
	34:2	716.5	0.44 ± 0.14*	0.55 ± 0.05		
	36:1	746.5	0.45 ± 0.17	0.54 ± 0.05	**0.23 ± 0.08**	**0.59 ± 0.05***
	36:2	744.5	0.30 ± 0.08	0.45 ± 0.04	0.32 ± 0.08	0.56 ± 0.05
	36:3	742.5	0.30 ± 0.09	0.53 ± 0.05	0.32 ± 0.10	0.73 ± 0.07
	36:4	740.5	0.34 ± 0.13	0.41 ± 0.04		
	38:3	770.5	0.31 ± 0.11	0.49 ± 0.05		
	38:4	768.5	0.30 ± 0.12	0.38 ± 0.03		
	38:5	766.5	0.35 ± 0.12	0.61 ± 0.05		
	38:6	764.5	0.41 ± 0.16	0.57 ± 0.05†		
	40:5	794.5	0.41 ± 0.16	0.54 ± 0.06		
	40:6	792.5	0.46 ± 0.13	0.61 ± 0.05		
Ether PE	P-16:0/20:4	724.5	0.29 ± 0.18	0.37 ± 0.04	0.39 ± 0.21	0.52 ± 0.06
	P-16:1/22:6	746.5	0.45 ± 0.18	0.39 ± 0.13*	**0.33 ± 0.1**	**0.58 ± 0.13**
	P-18:0/20:4	752.5	0.38 ± 0.30*	0.49 ± 0.05		
	P-18:1/20:4	750.5	0.38 ± 0.17	0.43 ± 0.04		
LPA	18:2	433.5			**0.38 ± 0.07**	**0.38 ± 0.03**
PI	16:0/18:2	833.5	**2.80 ± 0.31**	**1.53 ± 0.08**		
	16:0/20:4	857.5	**2.10 ± 0.52**	**1.76 ± 0.10**		
	18:0/20:3	887.5	**3.91 ± 0.61**	**2.20 ± 0.12**		
	18:1/18:0	863.5	**2.32 ± 0.25**	**1.86 ± 0.12**	0.39 ± 0.18	0.57 ± 0.04
DG	16:1_18:0	612.5	**2.66 ± 0.69**	**2.01 ± 0.34**		

supplementary Table S4. The isomeric structures of PC, PE, and TG are listed in supplementary Table S5. These results were carefully compared with those previously obtained under different run conditions ($t_G = 30$ min) using patient samples from a different group that was reported in an earlier study [7]. The differences in lipid profiles in the liver and gastric cancer groups compared with controls were illustrated using PCA plots (Fig. 4). The lipid profiles of individual samples (n = 50 each for the liver, gastric cancer, and control groups) using the optimised method ($t_G = 10$ min) were compared in plots with those obtained previously using $t_G = 30$ min (n = 20 for each group). Fig. 4b was regenerated from the raw data with permission from [7] (Copyright 2019 Elsevier B.V.). Both plots were based on lipids showing significant changes (>2-fold and $p < 0.05$) in both patient groups compared with the control group. Data points represent the individual human samples and appear to be clustered clearly for each group (gastric cancer, liver cancer, and control). There was some overlap between the gastric cancer and control groups observed in the previous study, which may be attributed to differences in the number of patient samples in the present study (50/each group) and the previous study (20/each group). In this study, plasma lipid patterns in both cancer groups are clearly different from each other and from the control. Although the two studies used different patient samples and different analytical methods, the overall grouping observed in the PCA plots are similar. Lipid alterations in the liver and gastric cancer groups were visualised in a heat map (supplementary Fig. S5), which was plotted for the specific lipid species that were significantly different between these groups (>3.0 fold differences and $p < 0.01$) according to the previous study. Similar to the observations in the previous study, LPC levels increased, while levels of LPE, PE, and PE plasmalogen species decreased in both cancer groups compared to in the control. The levels of PI species were generally higher in the liver cancer group, while PC and LPA levels were lower in the gastric cancer group than in the control.

The alterations in lipid profiles between the cancer groups were explored in-depth by measuring the relative amounts of selected lipids (27 in the liver cancer and 15 in the gastric cancer group), which were found to be significantly different (>2.0 fold and $p < 0.05$) in a previous report [7]. Table 1 lists the fold change comparison of each lipid species (11 species common to both cancers, 16 species unique to the liver cancer group, and 4 species unique to the gastric cancer group) in the previous and the present study. Statistical p values of most species in Table 1 were found to be <0.01, except for those with * as $p < 0.05$, and † as $p > 0.05$. A total of 25 lipid species in the liver cancer group were statistically different ($p < 0.05$) from the controls, 14 of which (excluding PE 34:1 and 38:6) were unique to liver cancer. In the gastric cancer group, all 15 species were significantly different from the controls, of which four species (3 PCs and 1 LPA) were unique to gastric cancer. The fold ratio of most lipid species obtained using the high-speed analysis method were similar to those obtained using the previous method, with a few exceptions: LPC 16:0 and 18:2 exhibited relatively low increases (<2 fold) in both cancer types using the high-speed method. The candidate lipid markers specific to each cancer reported in [7] were based on an area under curve (AUC) > 0.800 by receiver operating characteristic (ROC) analysis (Table 1). In the present study, ROC analysis was carried out for each candidate lipid molecule (7 for liver cancer and 9 for gastric cancer), and the AUC values between the two methods were compared (Table 2). In the liver cancer group, 6 out of 7 species had an AUC > 0.800 when using the high-speed method (Fig. 5). In the present sample group, LPC 16:0 was less upregulated (1.43 ± 0.05 vs. 4.55 ± 0.82) than in the previous sample group. In the case of gastric, lung, and colorectal cancer, 5 out of 9 (5/9), 4/6, and 6/7 candidates had AUC values >0.800, respectively (Table 2). Although the performance of the present high-speed quantification method ($t_G = 10$ min) is approximately 73% that of the comprehensive analysis ($t_G = 30$ min) in terms of the number of lipids with an AUC > 0.800, the present results show good selectivity in the four cancer groups, considering that different sample sets were employed in the two studies.

Table 2

Comparison of area under curve (AUC) values from receiver operating characteristic (ROC) analysis for the potential lipid biomarker candidates of the four cancer types between the present high-speed lipid quantification (t_G = 10 min) and the previous report (t_G = 30 min) [7]. Type of cancer is (a) liver, (b) gastric, (c) lung, and (d) colorectal cancer. * for $p < 0.05$, and ** for $p < 0.01$. Data from Ref. were reprinted with permission from [7]. Copyright 2019 Elsevier B.V.

Class	Molecular species	m/z	Fold ratio (L/C) in [7]	AUC	Fold ratio (L/C) by the present study	AUC
(a) Liver cancer						
LPC	16:0	496.5	4.55 ± 0.82**	1.000	1.43 ± 0.05**	0.721
	18:2	520.5	4.77 ± 1.10**	0.940	1.69 ± 0.07**	0.840
PI	16:0/18:2	833.5	2.80 ± 0.31**	0.810	1.53 ± 0.08**	0.802
	16:0/20:4	857.5	2.10 ± 0.52**	0.824	1.76 ± 0.10**	0.817
	18:0/20:3	887.5	3.91 ± 0.61**	0.974	2.20 ± 0.12**	0.960
	18:1/18:0	863.5	2.32 ± 0.25**	0.838	1.86 ± 0.12**	0.903
DG	16:1_18:0	612.5	2.66 ± 0.69**	0.833	2.01 ± 0.34**	0.803
Total				7		6

Class	Molecular species	m/z	Fold ratio (G/C) in [7]	AUC	Fold ratio (G/C) by the present study	AUC
(b) Gastric cancer						
PC	34:2	758.5	0.49 ± 0.03**	0.963	0.48 ± 0.02**	0.937
	36:4	782.5	0.48 ± 0.16**	0.979	0.49 ± 0.01**	0.938
	36:3	784.5	0.50 ± 0.10**	0.913	0.45 ± 0.01**	0.959
LPE	16:0	454.5	0.29 ± 0.08**	0.913	0.52 ± 0.07**	0.808
	18:0	482.5	0.48 ± 0.12**	0.905	0.57 ± 0.07**	0.784
	18:1	480.5	0.19 ± 0.06**	0.926	0.53 ± 0.07**	0.774
PE	36:1	746.5	0.23 ± 0.08**	0.874	0.59 ± 0.05*	0.650
PEp	P-16:1/22:6	746.5	0.33 ± 0.13**	0.845	0.58 ± 0.13**	0.544
LPA	18:2	433.5	0.38 ± 0.07**	0.924	0.38 ± 0.03**	0.840
Total				9		5

Class	Molecular species	m/z	Fold ratio (Lg/C) in [7]	AUC	Fold ratio (Lg/C) by the present study	AUC
(c) Lung cancer						
PE	38:3	770.5	0.32 ± 0.13**	0.835	0.60 ± 0.07**	0.826
PEp	P-18:1/20:4	750.5	0.34 ± 0.16**	0.879	0.37 ± 0.04**	0.964
SM	d18:1/20:0	787.5	0.33 ± 0.12**	0.912	0.59 ± 0.05**	0.890
LPI	16:0	571.5	4.66 ± 1.52**	0.912	2.13 ± 0.95**	0.794
TG	50:1	850.7	2.13 ± 0.32**	0.885	1.98 ± 0.20**	0.782
	54:4	900.7	3.90 ± 0.19*	0.894	1.85 ± 0.20**	0.850
Total				6		4

Class	Molecular species	m/z	Fold ratio (Col/C) in [7]	AUC	Fold ratio (Col/C) by the present study	AUC
(d) Colorectal cancer						
PC	36:2	786.5	0.46 ± 0.15*	0.925	0.32 ± 0.01**	0.988
	36:1	746.5	0.16 ± 0.06*	0.938	0.43 ± 0.05**	1.000
	38:4	768.5	0.15 ± 0.06*	0.916	0.43 ± 0.05**	0.757
	38:6	764.5	0.17 ± 0.07*	0.922	0.63 ± 0.06**	0.883
PEp	P-16:0/20:4	724.5	0.11 ± 0.06*	0.963	0.18 ± 0.02**	1.000
	P-18:0/20:4	752.5	0.15 ± 0.17*	0.963	0.44 ± 0.06**	0.998
	P-18:1/18:1	728.5	0.20 ± 0.16*	0.966	0.31 ± 0.09**	1.000
	P-18:1/22:4	778.5	0.24 ± 0.12*	0.953	0.11 ± 0.01**	0.948
Total				8		7

4. Conclusions

Lipidomic analysis must contend with the challenge of carrying out high-speed and high-throughput analysis of a large number of lipidome samples to develop disease-specific lipid markers. Due to the complicated nature of lipids, the LC-MS approach has been the essential, but rate-determining, step in comprehensive qualitative and quantitative lipidomic analyses. The present study optimised a high-speed analytical method utilising nUHPLC-ESI-MS/MS for lipid analysis by examining the influence of dwell time, column flow rate, initial MP composition, and gradient duration on lipid separation and detection by evaluating time-based separation efficiencies. By examining the capability to distinguish between isobaric species of an SM and a second isotope of PC, which have the same m/z values during SRM-based quantification, we can recommend that separation speed and loss of resolution should be balanced when pursuing high-speed lipid analysis. After method optimisation, the gradient time for lipid analysis could be reduced to 10 min without losing the resolution required for quantitative measurements.

The optimised high-speed method was evaluated by applying it to

plasma samples of patients with four different cancer types (liver, gastric, lung, and colorectal) to compare the differences in candidate lipid species that were identified in a previous study with a gradient time of 30 min (t_G) [7]. The two analytical methods showed similar patterns in the PCA plots of the liver and gastric cancer groups, and similar individual fold ratios (vs. control) of selected lipid species (Table 1), despite the use of samples from different patients in each study. A closer examination of the candidate lipid biomarkers (27 from liver cancer and 15 from gastric cancer, including 11 species common to both) that were previously selected (>2-fold difference, $p < 0.05$) in liver and gastric cancers [7] showed that the present high-speed method could quantify differences among 25 species in cancer samples compared to those in the controls. Most individual lipid species had similar fold ratio values between the two methods, except for two LPC species, which showed unexpectedly low increases in both cancer types in the present study's sample groups. A further examination of candidate lipid markers of each cancer type reported in this previous study [7] using ROC analysis showed that approximately 73% of the lipid candidates exhibited AUC values >0.800 using the present method (t_G = 10 min) compared with the previous study (t_G = 30 min): 6 out of 7 species in the liver cancer
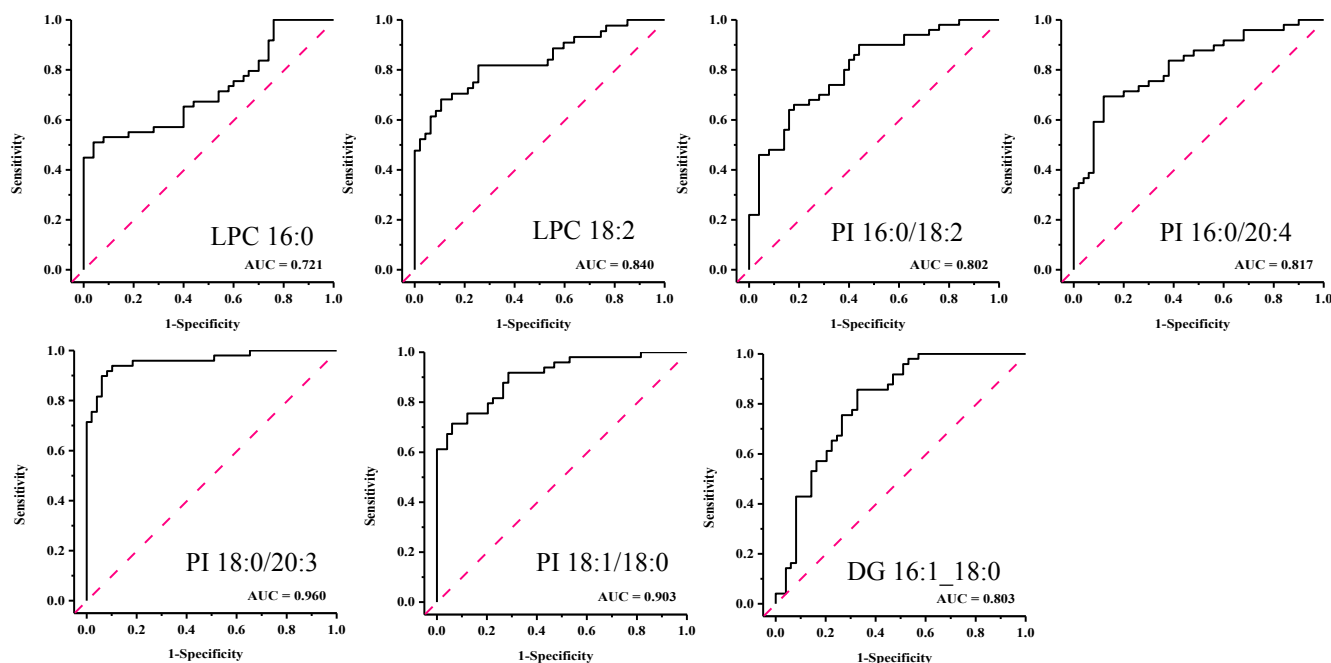
Fig. 5. Receiver operating characteristic (ROC) curves of the liver cancer specific lipid species obtained by the present high-speed lipid quantification method.

group, 5 out of 9 in the gastric cancer group, 4 out of 6 in the lung cancer group, and 6 out of 7 in the colorectal cancer group. In conclusion, a 10-min gradient duration with polarity switching can achieve rapid lipidome analysis by nUHPLC-ESI-MS/MS. This rapid method has potential applications in clinical settings, where decision-making for personalised medicine relies on the accurate measurement of panels of biomarkers.

CRediT authorship contribution statement

Gwang Bin Lee: Investigation, Methodology, Writing - original draft. **Young Beom Kim:** Formal analysis. **Jong Cheol Lee:** Data curation. **Myeong Hee Moon:** Supervision, Writing - review & editing.

Declaration of Competing Interest

The authors declare that they have no known competing financial interests or personal relationships that could have appeared to influence the work reported in this paper.

Acknowledgements

Funding

Appendix A. Supplementary material

Supplementary data to this article can be found online at https://doi.org/10.1016/j.jchromb.2021.122739.

References

[1] M.R. Wenk, The emerging field of lipidomics, Nat. Rev. Drug Discov. 4 (2005) 594–610.

[2] A. Bosio, E. Binczek, W. Stoffel, Molecular cloning and characterization of the mouse CGT gene encoding UDP-galactose ceramide-galactoysyltransferase (cerebroside synthetase), Genomics 35 (1996) 223–226.

[3] C.R. Santos, A. Schulze, Lipid metabolism in cancer, FEBS J. 279 (2012) 2610–2623.

[4] N.G. Forouhi, G. Jenkinson, E.L. Thomas, S. Mullick, S. Mierisova, U. Bhonsle, P. M. McKeigue, J.D. Bell, Relation of triglyceride stores in skeletal muscle cells to central obesity and insulin sensitivity in European and South Asian men, Diabetologia 42 (1999) 932–935.

[5] B.H. Goodpaster, F.L. Thaete, J.A. Simoneau, D.E. Kelley, Subcutaneous abdominal fat and thigh muscle composition predict insulin sensitivity independently of visceral fat, Diabetes 46 (1997) 1579–1585.

[6] T. Uehara, H. Kikuchi, S. Miyazaki, I. Iino, T. Setoguchi, Y. Hiramatsu, M. Ohta, K. Kamiya, Y. Morita, H. Tanaka, S. Baba, T. Hayasaka, M. Setou, H. Konno, Overexpression of Lysophosphatidylcholine Acyltransferase 1 and Concomitant Lipid Alterations in Gastric Cancer, Ann. Surg. Oncol. 23 (Suppl 2) (2016) S206–213.

[7] G.B. Lee, J.C. Lee, M.H. Moon, Plasma lipid profile comparison of five different cancers by nanoflow ultrahigh performance liquid chromatography-tandem mass spectrometry, Anal. Chim. Acta 1063 (2019) 117–126.

[8] Q.H. Xuan, F.J. Zheng, D. Yu, Y. Ouyang, X.J. Zhao, C.X. Hu, G.W. Xu, Rapid lipidomic profiling based on ultra-high performance liquid chromatography-mass spectrometry and its application in diabetic retinopathy, Anal. Bioanal. Chem. 412 (2020) 3585–3594.

[9] E. Fahy, S. Subramaniam, H.A. Brown, C.K. Glass, A.H. Merrill Jr., R.C. Murphy, C. R. Raetz, D.W. Russell, Y. Seyama, W. Shaw, T. Shimizu, F. Spener, G. van Meer, M. S. VanNieuwenhze, S.H. White, J.L. Witztum, E.A. Dennis, A comprehensive classification system for lipids, J. Lipid Res. 46 (2005) 839–861.

[10] R. Taguchi, J. Hayakawa, Y. Takeuchi, M. Ishida, Two-dimensional analysis of phospholipids by capillary liquid chromatography/electrospray ionization mass spectrometry, J. Mass Spectrom. 35 (2000) 953–966.

[11] G. Isaac, D. Bylund, J.E. Mansson, K.E. Markides, J. Bergquist, Analysis of phosphatidylcholine and sphingomyelin molecular species from brain extracts using capillary liquid chromatography electrospray ionization mass spectrometry, J. Neurosci. Methods 128 (2003) 111–119.

[12] O. Fiehn, J. Kim, Metabolomics insights into pathophysiological mechanisms of interstitial cystitis, Int. Neurourol. J. 18 (2014) 106–114.

[13] H.H. Bui, J.K. Leohr, M.S. Kuo, Analysis of sphingolipids in extracted human plasma using liquid chromatography electrospray ionization tandem mass spectrometry, Anal. Biochem. 423 (2012) 187–194.

[14] H.C. Yeo, S.W. Chen, Y.S. Ho, D.Y. Lee, An LC-MS-based lipidomics pre-processing framework underpins rapid hypothesis generation towards CHO systems biotechnology, Metabolomics 14 (2018) 98–110.

[15] T. Hou, M.C. Taylor, P. Shrestha, S. Singh, Z.-J. Zhang, X.-R. Zhou, Liquid chromatography-mass spectrometry based approach for rapid comparison of lysophosphatidic acid acyltransferase activity on multiple substrates, J. Chromatogr. A 1572 (2018) 100–105.

[16] Q. Zhang, H.R. Xu, R. Liu, P. Gao, X. Yang, W. Jin, Y.W. Zhang, K.S. Bi, Q. Li, A Novel Strategy for Targeted Lipidomics Based on LC-Tandem-MS Parameters Prediction, Quantification, and Multiple Statistical Data Mining: Evaluation of Lysophosphatidylcholines as Potential Cancer Biomarkers, Anal. Chem. 91 (2019) 3389–3396.

[17] J. Franco, C. Ferreira, T.J.P. Sobreira, J.P. Sundberg, H. HogenEsch, Profiling of epidermal lipids in a mouse model of dermatitis: Identification of potential biomarkers, PLoS ONE 13 (2018).

[18] M. Navarro-Reig, R. Tauler, G. Iriondo-Frias, J. Jaumot, Untargeted lipidomic evaluation of hydric and heat stresses on rice growth, J. Chromatogr. B 1104 (2019) 148–156.

[19] A. Basit, D. Piomelli, A. Armirotti, Rapid evaluation of 25 key sphingolipids and phosphosphingolipids in human plasma by LC-MS/MS, Anal. Bioanal. Chem. 407 (2015) 5189–5198.

[20] Y.Y. Zhao, H. Miao, X.L. Cheng, F. Wei, Lipidomics: Novel insight into the biochemical mechanism of lipid metabolism and dysregulation-associated disease, Chem. Biol. Interact. 240 (2015) 220–238.

[21] O.L. Knittelfelder, B.P. Weberhofer, T.O. Eichmann, S.D. Kohlwein, G. N. Rechberger, A versatile ultra-high performance LC-MS method for lipid profiling, J. Chromatogr. B Analyt. Technol. Biomed. Life Sci. 951–952 (2014) 119–128.

[22] S.K. Byeon, J.C. Lee, B.C. Chung, H.S. Seo, M.H. Moon, High-throughput and rapid quantification of lipids by nanoflow UPLC-ESI-MS/MS: application to the hepatic lipids of rabbits with nonalcoholic fatty liver disease, Anal. Bioanal. Chem. 408 (2016) 4975–4985.

[23] J.C. Lee, I.Y. Kim, Y. Son, S.K. Byeon, D.H. Yoon, J.S. Son, H.S. Song, W. Song, J. K. Seong, M.H. Moon, Evaluation of treadmill exercise effect on muscular lipid profiles of diabetic fatty rats by nanoflow liquid chromatography-tandem mass spectrometry, Sci. Rep. 6 (2016) 29617.

[24] S.M. Park, S.K. Byeon, H. Sung, S.Y. Cho, J.K. Seong, M.H. Moon, Lipidomic Perturbations in Lung, Kidney, and Liver Tissues of p53 Knockout Mice Analyzed by Nanoflow UPLC-ESI-MS/MS, J. Proteome Res. 15 (2016) 3763–3772.

[25] J.S. Yang, J.C. Lee, S.K. Byeon, K.H. Rha, M.H. Moon, Size Dependent Lipidomic Analysis of Urinary Exosomes from Patients with Prostate Cancer by Flow Field-Flow Fractionation and Nanoflow Liquid Chromatography-Tandem Mass Spectrometry, Anal. Chem. 89 (2017) 2488–2496.

[26] D.Y. Bang, S.K. Byeon, M.H. Moon, Rapid and simple extraction of lipids from blood plasma and urine for liquid chromatography-tandem mass spectrometry, J. Chromatogr. A 1331 (2014) 19–26.

[27] P. Petersson, A. Frank, J. Heaton, M.R. Euerby, Maximizing peak capacity and separation speed in liquid chromatography, J. Sep. Sci. 31 (2008) 2346–2357.

[28] J.C. Giddings, Unified Separation Science, John Wiley & Sons Inc, New York, 1991.